

Local Differential Privacy for Federated Learning in Industrial Settings

M.A.P. Chamikara^{*†}, Dongxi Liu^{*}, Seyit Camtepe^{*}, Surya Nepal^{*}, Marthie Grobler^{*}, Peter Bertok[‡], and Ibrahim Khalil[‡]

^{*}CSIRO's Data61, Australia

[†]Cyber Security Cooperative Research Centre, Australia

[‡]RMIT University, Australia

Abstract—Federated learning (FL) is a collaborative learning approach that has gained much attention due to its inherent privacy preservation capabilities. However, advanced adversarial attacks such as membership inference and model memorization can still make FL vulnerable and potentially leak sensitive private data. Literature shows a few attempts to alleviate this problem by using global (GDP) and local differential privacy (LDP). Compared to GDP, LDP approaches are gaining more popularity due to stronger privacy notions and native support for data distribution. However, DP approaches assume that the server that aggregates the models, to be honest (run the FL protocol honestly) or semi-honest (run the FL protocol honestly while also trying to learn as much information possible), making such approaches unreliable for real-world settings. In real-world industrial environments (e.g. healthcare), the distributed entities (e.g. hospitals) are already composed of locally running machine learning models (e.g. high-performing deep neural networks on local health records). Existing approaches do not provide a scalable mechanism to utilize such settings for privacy-preserving FL. This paper proposes a new local differentially private FL (named LDPFL) protocol for industrial settings. LDPFL avoids the requirement of an honest or a semi-honest server and provides better performance while enforcing stronger privacy levels compared to existing approaches. Our experimental evaluation of LDPFL shows high FL model performance (up to $\sim 98\%$) under a small privacy budget (e.g. $\epsilon = 0.5$) in comparison to existing methods.

Index Terms—Federated Learning, distributed machine learning, differential privacy, local differential privacy, privacy preserving federated learning, privacy preserving distributed machine learning.

I. INTRODUCTION

Server-centric machine learning (ML) architectures cannot address the massive data distribution in the latest technologies utilized by many industries, including healthcare and smart agriculture. Besides, collecting data from such industries to one central server for ML introduces many privacy concerns [1]. Federated learning (FL) is a recently developed distributed machine learning approach that provides an effective solution to privacy-preserving ML [2]. In a distributed environment, FL enables the clients to collect and process data to train a local ML model. The clients are then only required to share the model parameters of the locally trained ML models with a central server for parameter aggregation to generate a global representation of all client models. Finally, the server shares the global model with all participating clients. In this way, FL bypasses the necessity of sharing raw data with any

other party involved in the ML training process. However, the model parameters of the locally shared models can still leak private information under certain conditions [3], [4]. Hence, FL on sensitive data such as biometric images, health records, and financial records still poses privacy risks if proper privacy-preservation mechanisms are not imposed.

Different approaches based on cryptographic scenarios and noise addition (randomization) mechanisms have been developed to mitigate the privacy leaks associated with FL [4], [5]. For example, secure multi-party computation (SMC) and homomorphic encryption are two of FL's most frequently tested cryptographic approaches. However, cryptographic approaches tend to reduce FL performance drastically due to their high computational complexity, and most SMC approaches need a large number of communications that further reduce the efficiency of FL [5], [6]. Furthermore, most cryptographic approaches for FL privacy need to assume semi-honest (honest but curious) computations at certain points of the FL process. A semi-honest entity is assumed to conduct computations honestly; however, curious to learn as much information possible [7]. Among noise addition approaches, differentially private approaches are more preferred due to the robust privacy guarantees [4], [8]. Differentially private approaches entail a certain decline of accuracy due to the noise addition; however, the performance gain due to enabling calculations on data in their original configurations/formats, compared to cryptographic protocols generating long encrypted strings, makes DP approaches preferred for large-scale machine learning scenarios such as FL [1].

Existing DP approaches can be categorized into global differential privacy (GDP) [9], [10] and local differential privacy (LDP) [1] based on the noise application mechanism. In GDP, a trusted curator applies calibrated noise [11], [12], whereas, in LDP, the data owner perturbs their data before releasing them for any third party [12]. LDP provides higher levels of privacy as it imposes more noise compared to GDP, whereas GDP provides better utility due to less amount of noise imposed on the privacy preservation process [1]. Most existing approaches for FL are based on GDP [8]. However, the requirement of a trusted party makes GDP approaches less practical, whereas LDP approaches provide a more practical way of dealing with the distributed clients in FL. The existing approaches try to impose LDP by applying noise/random-

ization over the model parameters of the local models [13]. However, most of these LDP approaches for FL cannot control the privacy budgets efficiently due to the extreme dimensionality of parameter matrices of underlying deep learning models [13]. For example, the LDP approach for FL proposed in [4] utilizes extensive ϵ values to enable sufficient utility challenging its use in practical settings. Besides, existing LDP approaches are not rigorously tested against more complex datasets [4], [14]. Besides, the weight distribution in different layers of the models has not been explicitly considered during the application of LDP [13].

In this paper, we propose a novel local differentially private federated learning approach (named LDPFL: Local Differential Privacy for Federated Learning) that mitigates the issues of existing approaches. LDPFL solves the complexity of applying LDP over high dimensional parameter matrices by applying randomization over a 1D vector generated from the intermediate output of a locally trained model. LDPFL applies randomization over this 1D vector and trained a second fully connected deep neural network as the client model of an FL setting. The randomization mechanism in LDPFL utilizes randomized response (RR) [15] and optimized unary encoding (OUE) [16] to guarantee differential privacy of FL. RR is a popular survey response randomization mechanism that guarantees DP, whereas OUE is a utility enhancement of differentially private binary code randomization. Since LDPFL randomizes the inputs to the local models rather than altering the weights of the local models, LDPFL can provide better flexibility in choosing randomization, privacy composition, and model convergence compared to existing LDP approaches for FL. Compared to previous approaches (SMC [6], [14], GDP - DPSGD) [10], [14], and LDP - α -CLDP-Fed [14], [17]), our empirical analysis shows that LDPFL achieves excellent accuracy under extreme cases of privacy budgets (e.g. $\epsilon = 0.5$), ensuring a minimal privacy leak.

The rest of the paper is organized as follows. The preliminaries of the proposed work are presented in Section II. Section III explains the steps of the proposed approach. Section IV provides the results and discussions of the proposed work. A summary of related works is provided in Section V. Section VI provides the conclusion of the paper.

II. BACKGROUND

This section provides brief descriptions of the preliminaries used in LDPFL that were proposed for privacy-preserving federated learning on deep learning (e.g. convolutional neural networks). LDPFL utilizes the concepts of local differential privacy (LDP) - a type of differential privacy, randomized response (an LDP protocol), Randomized Aggregatable Privacy-Preserving Ordinal Response - RAPPOR (an LDP protocol based on randomized response for binary vectors), and optimized unary encoding (which is an optimization on RAPPOR for better utility).

A. Federated Learning

Federated learning is a distributed machine learning approach to train a global model on data distributed over multiple locations without sharing the row data between contributing parties [18]. FL involves N distributed parties agreed on training local DNN models with the same configuration. The process starts with a central server randomly initializing the model parameters, \mathcal{M}_0 , and distributing them with the clients to initialize their copy of the model. The clients train their local model separately using the data in their local repository for several local epochs and share the updated model parameters, M_u , with the server. The server aggregates the model parameters received from all clients using an aggregation protocol such as federated averaging to generate the federated model (\mathcal{ML}_{fed}). Equation 1 shows the process of federated averaging (calculating the average of values in each index of parameter matrices) to generate (\mathcal{ML}_{fed}), where $M_{u,i}$ represents the updated model parameters sent by i^{th} client. This is called one federation round. FL conducts multiple federation rounds until (\mathcal{ML}_{fed}) converges or the pre-defined number of rounds is reached. It was shown that (\mathcal{ML}_{fed}) produces accuracy as almost as close to a model centrally trained with the same data [19].

$$\mathcal{ML}_{fed} = \frac{1}{N} \sum_i M_{u,i} \quad (1)$$

B. Differential Privacy

Differential privacy (DP) is a privacy model that defines the bounds to how much information of data owners of a database should be revealed to an analyst [20]. These bounds are defined in terms of two parameters termed as the privacy budget/privacy loss (ϵ) and probability to fail/probability of error (δ). These two parameters together define the level of privacy enforced by the corresponding differentially private algorithm [20]. ϵ provides an insight into the privacy loss incurred during the application of the differentially private algorithm, and δ is the probability of a bad event happening. For n number of records, $\delta = 1/100 \times n$ mean that the chance of a bad event is 1%. Hence, δ should be maintained at a low value. Take x and y to be two adjacent datasets of the dataset D , where x differs from y only by one person. Assume that the datasets x and y as being collections of records from a universe \mathcal{X} and \mathbb{N} denotes the set of all non-negative integers, including zero. Then M satisfies (ϵ, δ) -differential privacy if Equation (2) holds.

Definition 1. A randomized algorithm M with domain $\mathbb{N}^{|\mathcal{X}|}$ and range R : is (ϵ, δ) -differentially private for $\delta \geq 0$ if for every adjacent datasets $x, y \in \mathbb{N}^{|\mathcal{X}|}$ and for any subset $S \subseteq R$,

$$Pr[(M(x) \in S)] \leq \exp(\epsilon)Pr[(M(y) \in S)] + \delta \quad (2)$$

C. Local Differential Privacy

The generic algorithmic approach of differential privacy is called the global differential privacy (GDP), which requires a

trusted curator to apply calibrated noise on the global statistics (e.g. query outputs) [21]. Local differential privacy (LDP) is the setting where the data owners apply randomization (or noise) on the input data before the data curator has access to them. However, LDP often produces too noisy data compared to GDP as each entry of the input dataset is randomized to achieve individual data owner-level privacy. LDP provides a better privacy notion compared to GDP due to the increased noise levels and nonnecessity of a trusted curator. Hence, LDP is deemed to be the state-of-the-art approach for privacy-preserving data collection and distribution. A randomized algorithm A provides ε -local differential privacy if Equation (3) holds [22].

Definition 2. A randomized algorithm A satisfies ε -local differential privacy if for all pairs of client's values v_1 and v_2 and for all $Q \subseteq \text{Range}(A)$ and for $(\varepsilon \geq 0)$, Equation (3) holds. $\text{Range}(A)$ is the set of all possible outputs of the randomized algorithm A .

$$\Pr[A(v_1) \in Q] \leq \exp(\varepsilon) \Pr[A(v_2) \in Q] \quad (3)$$

D. Randomized Response

Randomized response is one of the most basic LDP algorithms that was initially introduced to eliminate evasive answer biases in survey responses of "yes" or "no" answers [23]. The randomization is done based on the outcome of flipping an unbiased coin. If the coin flip outcome is "heads", the true answer is recorded. If the coin flip outcome is "tails", the coin is flipped again to answer "Yes" if it turns up "heads"; otherwise, the answer is recorded as "No". Randomized response provides ε -differential privacy where $p = e^\varepsilon / (1 + e^\varepsilon)$ is the probability of a user providing an answer truthfully when a biased coin is used [12].

E. Randomized Aggregatable Privacy-Preserving Ordinal Response (RAPPOR)

RAPPOR is an LDP algorithm proposed by Google based on the problem of estimating a client-side distribution of string values drawn from a discrete data dictionary [22]. One of the applications of RAPPOR includes tracing the distribution of browser configuration strings in Chrome web browser belonging to many users. RAPPOR takes an input, v_i , that is encoded into a binary string. Each input v_i is encoded as a vector of d bits, and each d -bit vector contains $d - 1$ zeros and one bit of 1s. Next, $\mathbf{B}[v_i]$ is randomized to obtain, $\mathbf{B}'[v_i]$ satisfying DP.

F. Sensitivity of the encoded binary string

The sensitivity of the encoded inputs (binary strings) to an LDP process that is based on transferring bit strings determines the level of randomization necessary on the input data to enforce DP. The sensitivity, Δf of a function, f is considered to be the maximum influence that a single individual can have on f . This can be represented as given in Equation (4), where x and y are two neighboring datasets in GDP or two adjacent

inputs in LDP. $\|\cdot\|_1$ represents the $L1$ norm of a vector [24]. For example, Δf , in RAPPOR is 2 as the maximum difference between two adjacent encoded bit strings ($\mathbf{B}[v_i]$ and $\mathbf{B}[v_{i+1}]$) is only two bits.

$$\Delta f = \max\{\|f(x) - f(y)\|_1\} \quad (4)$$

G. Bit randomization probability in an LDP algorithm

Let us consider the bit randomization scenario utilized in RAPPOR to quantify the probability of randomization of an LDP process that is based on transferring bit strings. Take p to be the probability of preserving the true value of an original bit in an input bit-string. p follows Equation (5), where ε is the privacy budget offered by the LDP process [22], [25].

$$p = \frac{e^{\frac{\varepsilon}{2}}}{1 + e^{\frac{\varepsilon}{2}}} = \frac{e^{\frac{\varepsilon}{2}}}{1 + e^{\frac{\varepsilon}{2}}} \quad (5)$$

H. Optimized Unary Encoding

Assume that the binary encoding used in RAPPOR (also referred to as Unary Encoding [16]) encodes an input instance v_i into its binary representation B , which is a d bit binary vector. Let $B[i]$ represents the i^{th} bit and $B'[i]$ is the perturbed i^{th} bit. Assume that, only the j^{th} position of B is set to 1, whereas the other bits are set to zero. Unary Encoding (UE) [22] perturbs the bits of B according to Equation 6.

$$\Pr[B'[i] = 1] = \begin{cases} p, & \text{if } B[i] = 1 \\ q, & \text{if } B[i] = 0 \end{cases} \quad (6)$$

UE satisfies ε -LDP [16], [22] for,

$$\varepsilon = \ln \left(\frac{p(1-q)}{(1-p)q} \right) \quad (7)$$

This can be proven as done in [16], [22] for any inputs v_1 , v_2 , and output B with sensitivity = 2.

Proof. Considering a sensitivity of 2, choose p and q as follows,

$$p = \frac{e^{\frac{\varepsilon}{2}}}{1 + e^{\frac{\varepsilon}{2}}} \quad (8)$$

$$q = \frac{1}{1 + e^{\frac{\varepsilon}{2}}} \quad (9)$$

$$\begin{aligned} \frac{\Pr[\mathbf{B}[v_1]]}{\Pr[\mathbf{B}[v_2]]} &= \frac{\prod_{i \in [d]} \Pr[\mathbf{B}[i]|v_1]}{\prod_{i \in [d]} \Pr[\mathbf{B}[i]|v_2]} \\ &\leq \frac{\Pr[\mathbf{B}[v_1] = 1|v_1] \Pr[\mathbf{B}[v_2] = 0|v_1]}{\Pr[\mathbf{B}[v_1] = 1|v_2] \Pr[\mathbf{B}[v_2] = 0|v_2]} \quad (10) \\ &= \frac{p}{q} \cdot \frac{1-q}{1-p} = e^\varepsilon \end{aligned}$$

Each bit is flipped independently. Equation 10, represents the state where v_1 and v_2 result in bit-vectors that differ only in locations v_1 and v_2 . The maximum of this ratio is when v_1 is 1 and v_2 is 0 as represented by Equation 10. \square

Optimized Unary Encoding (OUE) introduces a utility enhancement to Unary Encoding by perturbing 0s and 1s differently. When B is a long binary vector, the number of 0s is significantly greater than the number of 1s in B . OUE introduces a mechanism to reduce the probability of perturbing 0 to 1 ($p_{0 \rightarrow 1}$). By setting $p = \frac{1}{2}$ and $q = \frac{1}{1+e^\epsilon}$, OUE improves the budget allocation for transmitting the 0 bits in their original state as much as possible. We can show that OUE provides ϵ -LDP when $p = \frac{1}{2}$, $q = \frac{1}{1+e^\epsilon}$, and sensitivity = 2 as shown in Equation 7.

Proof. Considering a sensitivity of 2, define,

$$p = \frac{1}{2} \quad (11)$$

$$q = \frac{1}{1+e^\epsilon} \quad (12)$$

$$\begin{aligned} \frac{\Pr[\mathbf{B}|v_1]}{\Pr[\mathbf{B}|v_2]} &= \frac{\prod_{i \in [d]} \Pr[\mathbf{B}[i]|v_1]}{\prod_{i \in [d]} \Pr[\mathbf{B}[i]|v_2]} \\ &\leq \frac{\Pr[\mathbf{B}[v_1] = 1|v_1] \Pr[\mathbf{B}[v_2] = 0|v_1]}{\Pr[\mathbf{B}[v_1] = 1|v_2] \Pr[\mathbf{B}[v_2] = 0|v_2]} \quad (13) \\ &= \frac{p}{q} \cdot \frac{1-q}{1-p} = e^\epsilon \end{aligned}$$

□

I. Postprocessing invariance/robustness and composition

Any additional computations on the outcomes of a DP algorithm do not weaken its privacy guarantees. This property is called the postprocessing invariance/robustness in DP. A processed outcome of a ϵ -DP algorithm still provides ϵ -DP. Composition is another property of DP that captures the degradation of privacy when multiple differentially private algorithms are performed on the same or overlapping datasets [26]. When two DP algorithms ϵ_1 -DP and ϵ_2 -DP are applied to the same or overlapping datasets, the union of the results is equal to $(\epsilon_1 + \epsilon_2)$ -DP [26]. In parallel composition, if a set of DP algorithms (M_1, M_2, \dots, M_n) are applied on a dataset D divided into disjoint subsets of D_1, D_2, \dots, D_n , respectively (so that M_i provides $\epsilon_i - DP$ for every D_i), the whole process will provide $\max\{\epsilon_1, \epsilon_2, \dots, \epsilon_n\} - DP$ on the entire dataset [27].

J. Convolutional Neural Networks (CNN)

A convolutional neural network (CNN) is a class of deep neural networks that uses a collection of layers named convolution layers with large receptive fields that enable powerful pattern recognition capabilities. *Pooling* is a function used to reduce the high dimensionality from each convolution layer to the next. The final pooled output from the last convolution layer is a sizeable 1-D vector [28]. This 1-D vector is then passed through a fully connected network for the classification of the inputs (e.g. images).

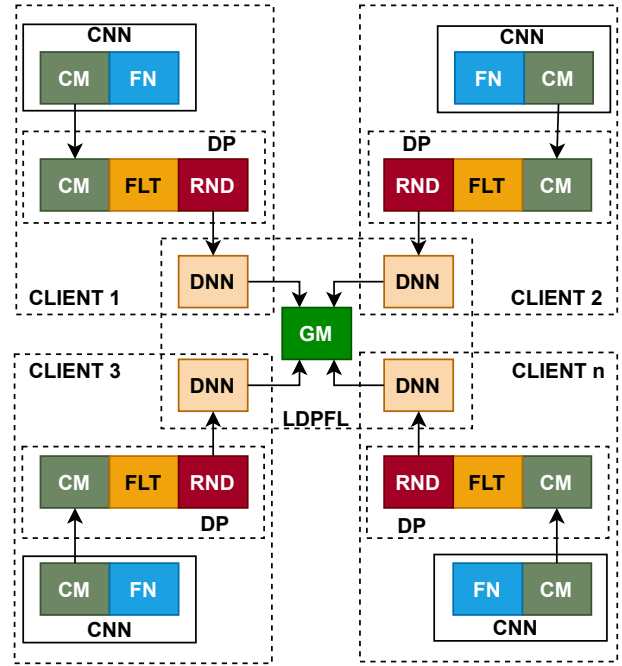


Figure 1: The architecture of LDPFL. **CNN**: convolutional neural network **CM**: convolutional module of the CNN, **FN**: fully connected network module of the CNN, **FLT**: input flattening layer, **RND**: randomization layer, **DNN**: deep neural network, **GM**: parameter federated global model.

III. OUR APPROACH

This section provides the steps employed in enforcing differential privacy in federated learning based on local differential privacy in answering the issues (maintaining a proper balance between privacy and utility) of existing DP approaches for FL raised in Section I. The proposed approach is abbreviated as LDPFL (Local Differential Privacy for Federated Learning) solves. Fig. 1 shows the architecture of LDPFL. A client in LDPFL has three main tasks; (1) Generating a CNN converged on local data, (2) Generating flattened 1-D vectors of inputs and randomizing them to enforce DP (3) Federated Learning. In the proposed setting, we assume the clients to be large-scale entities such as banks and hospitals, and any data owner would share private data with only one entity in the distributed setting (this is to emulate the I.I.D setting). Each client has their learning setup where fully trained models are maintained on locally-owned private data. Hence, the clients are assumed to have large enough representative datasets to train their local models. However, to better generalize their models, the clients need to collaborate with other related entities (hospitals with other hospitals working on similar domains of data). Next, each client uses their fully trained CNNs to obtain flattened vectors of the input instances, which are then encoded to binary vectors and randomized to enforce DP. The randomized inputs are then used to train a global model (DM) using federated learning. The flow of the main steps of LDPFL is represented in Figure 2. The following sections provide

detailed descriptions of the executions of the corresponding steps.

A. Generating a fully trained CNN using the local data

Each client trains a fully populated CNN model (refer to **CNN** in Fig. 1) on the locally available data that enables local ML insights. We assume that all clients use the same architectural configurations for their local CNN models to maintain uniform dimensions. In the second step, the clients have to use the trained local CNN models to generate the flattened 1-D vectors of the inputs before input encoding and randomization. The randomized input vectors need to be of the same size for the FL setup. Besides, all clients must use the same CNN configurations for the input instances to be filtered through the same architecture of trained convolutional layers, allowing a uniform feature extraction procedure by the convolutional layers in all clients.

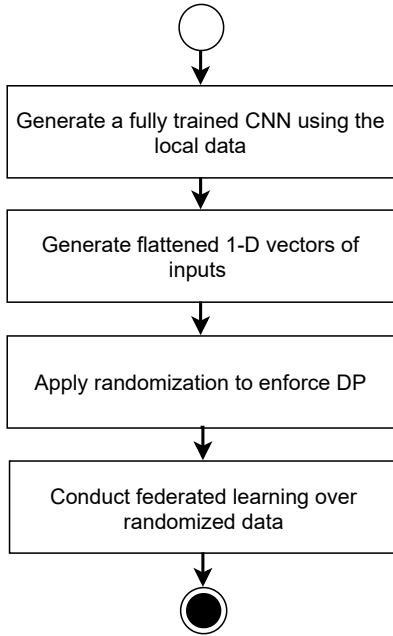


Figure 2: The flow of main steps in LDPFL.

B. Generating flattened 1-D vectors of inputs and randomizing them to enforce DP

Once the CNN models converge on the locally available datasets, the clients use the Convolution module (refer to **CM** in Fig. 1) of the converged CNN models to predict 1-D flattened outputs from the last convolutional layer of the **CM** for all inputs. Next, the predicted flattened outputs (1-D vectors: *1DV*) are encoded to binary vectors, which are then randomized to produce DP binary vectors. Utilizing a fully trained client CNN model for data flattening enables LDPFL to preserve the representative features of the input data and maintain the attribute distributions to generate high utility.

1) *Binary encoding*: Each element of a *1DV* is converted to a binary number according to Equation (14). m and n are the numbers of binary digits of the whole number and the

fraction, respectively. x represents the original input value where $x \in \mathbb{R}$, and $g(i)$ represents the i^{th} bit of the binary string where the least significant bit is represented when $k = -m$. Positive numbers are represented with a sign bit of 0, and negative numbers are represented with a sign bit of 1.

$$g(i) = \left(\left[2^{-k} x \right] \bmod 2 \right)_{k=-m}^n \quad \text{where } i = k + m \quad (14)$$

Algorithm 1: LDPFL Algorithm

Input:

$\{cx_1, \dots, cx_j\}$	\leftarrow	client datasets
ε	\leftarrow	privacy budget
m	\leftarrow	number of bits for the whole number of the binary representation
n	\leftarrow	number of bits for the fraction of the binary representation
α	\leftarrow	privacy budget coefficient
el	\leftarrow	the total number of local epochs
E	\leftarrow	the total number of global rounds

Output:

$GM \leftarrow$ differentially private global federated model

- 1 **Part I: Randomized data generation at clients:**
 - 2 Declare client model (CM_i) (refer to Section III-A);
 - 3 Train the CM_i with cx_i until the convergence;
 - 4 Split the trained CM_i to CNM_i and FN (refer to Section III-B);
 - 5 Declare, $l = (m + n + 1)$;
 - 6 Feed cx_i to the CNM_i and generate the sequence of 1-D feature arrays $\{d_1, \dots, d_j\}$;
 - 7 Convert each field (x) of d_q (where, $q = 1, \dots, j$) to binary using, $g(i) = \left(\left[2^{-k} |x| \right] \bmod 2 \right)_{k=-m}^n$ where, $i = k + m$;
 - 8 Generate array $\{b_1, \dots, b_j\}$ of the merged binary arrays for the elements in $\{d_1, \dots, d_j\}$;
 - 9 Calculate randomization probability according to Eq. 17;
 - 10 Randomize each element of $\{b_1, \dots, b_j\}$ using UER (refer Theorem 2) with probability p to generate $\{pb_1, \dots, pb_j\}$;
 - 11 Declare client model - DNN (CFM_i) for FL (refer to Section III-C);
 - 12 **Part II: Federated learning:**
 - 13 Server randomly initialize model parameters (M_0);
 - 14 Server sends M_0 to the clients;
 - 15 Clients initialize CFM_i using M_0 ;
 - 16 $e = 1$;
 - 17 **while** $e \leq E$ **do**
 - 18 **for each client, c_i of n clients in current round do**
 - 19 Train CFM_i using $\{pb_1, \dots, pb_j\}$ for el epochs;
 - 20 Send updated parameters $M_{u,i}$ to the server;
 - 21 Conduct federated averaging, $\mathcal{ML}_{fed} = \frac{1}{n} \sum_i \mathcal{M}_{u,i}$;
 - 22 Send \mathcal{ML}_{fed} to each c_i in the current round;
 - 23 $e = e + 1$;
 - 24 $GM = \mathcal{ML}_{fed}$;
 - 25 **return** GM ;
-

The binary conversion's sensitivity and precision (the range of floating values represented by the binary numbers) can be changed by increasing or decreasing the values chosen for n and m . Before the randomization, we merge all binary values into one long binary vector (L_{bv}) to consume the privacy

budget of randomization efficiently, as separately randomizing each binary value adds up the privacy budget after each randomization step according to the composition property of DP (refer to Section II-I). Large values for n and m can result in undesirably long binary vectors for randomization. Hence, n and m must be chosen carefully by empirically evaluating and adjusting them to produce high model accuracy.

2) *Randomization*: The length of an encoded binary string is $l = (m + n + 1)$; hence, the full length of the merged binary string (L_{bv}) is rl , where r is the total number of outputs of the $1DV$. Consequently, the sensitivity of the encoded binary strings can be taken as $l \times r$ as two consecutive inputs can differ by at most $l \times r$ bits. Now the probability of randomization can be given by Equation (15).

$$p = \frac{e^{\varepsilon/rl}}{1 + e^{\varepsilon/rl}} \quad (15)$$

With the p probability of randomization, the probability of randomization in reporting opposite of the true bits is $(1 - p) = \frac{1}{1 + e^{\varepsilon/rl}}$, which can lead to an undesirable level of randomization due to the extremely high sensitivity rl . To improve the utility of randomization, we employ an optimized randomization mechanism based on OUE, which perturbs 0s and 1s differently to reduce the probability of perturbing 0 to 1. LDPFL tries to optimize the randomization probabilities so that the utility can be maintained at a high level under the high sensitivity due to a large number of 1s available in the concatenated binary vector, L_{bv} . The parameter, α (the privacy budget coefficient) is introduced as defined in Theorem 1 to improve the flexibility of the probability selection further while still guaranteeing $\varepsilon - LDP$. By increasing α , we can increase the probability of transmitting the 0 bits in their original state.

Theorem 1. Modified OUE (MOUE)

When $\Pr[\mathbf{B}[v_1] = 1|v_1] = \frac{1}{1+\alpha}$, $\Pr[\mathbf{B}[v_1] = 1|v_2] = \frac{\alpha}{1+\alpha}$, $\Pr[\mathbf{B}[v_1] = 1|v_2] = \frac{\alpha e^{\frac{\varepsilon}{rl}}}{1+\alpha e^{\frac{\varepsilon}{rl}}}$, $\Pr[\mathbf{B}[v_2] = 0|v_2] = \frac{1}{1+\alpha e^{\frac{\varepsilon}{rl}}}$, and v_1 is 1 and v_2 is 0, the randomization provides $\varepsilon - LDP$.

Proof. The privacy budget (ε) is divided by rl for the randomization of each bit.

Then,

$$\begin{aligned} \frac{\Pr[\mathbf{B}[v_1]]}{\Pr[\mathbf{B}[v_2]]} &= \frac{\prod_{i \in [d]} \Pr[\mathbf{B}[i]|v_1]}{\prod_{i \in [d]} \Pr[\mathbf{B}[i]|v_2]} \\ &\leq \left(\frac{\Pr[\mathbf{B}[v_1] = 1|v_1] \Pr[\mathbf{B}[v_2] = 0|v_1]}{\Pr[\mathbf{B}[v_1] = 1|v_2] \Pr[\mathbf{B}[v_2] = 0|v_2]} \right)^{rl} \\ &= \left(\left(\frac{1}{1+\alpha} \right) \cdot \left(\frac{\alpha e^{\frac{\varepsilon}{rl}}}{1+\alpha e^{\frac{\varepsilon}{rl}}} \right) \right)^{rl} = e^{\varepsilon} \end{aligned} \quad (16)$$

□

Although MOUE provides flexibility in selecting the randomization probabilities, it can result in an undesirable level of randomization on 1s when α is large. Hence, MOUE

is further extended to impose extended flexibility over bit randomization by employing two randomization models over the bits of L_{bv} , by randomizing one half of the bit string (L_{bv}) differently from the other half while still preserving $\varepsilon - DP$ as defined in Theorem 2. Consequently, UER applies less randomization on $\frac{3}{4}$ of the binary string while $\frac{1}{4}$ of the binary string is heavily randomized. Hence, when UER randomizes long binary strings (e.g. 10,000 bits) with high sensitivity, it can maintain a high utility of the binary strings towards its applications as a significant part of the binary string is still preserved.

Theorem 2. (Utility enhancing randomization (UER))

Let $p(\mathbf{B}[i]v)$ be the probability of randomizing the i^{th} bit of the binary encoded string of v . For any inputs v_1, v_2 with a sensitivity = rl , define the probability, $p(\mathbf{B}[i]v)$ as in Equation 17. Then the randomization provides $\varepsilon - LDP$, when v_1 is 1 and v_2 is 0.

Proof. Considering a sensitivity of rl , choose the randomization probabilities according to Equation 17.

$$p(\mathbf{B}[i]v) = \begin{cases} \Pr[\mathbf{B}[v_1] = 1 | v_1] = \frac{\alpha}{1+\alpha} & \text{if } i \in 2n; n \in \mathbb{N} \\ \Pr[\mathbf{B}[v_2] = 0 | v_1] = \frac{\alpha e^{\frac{\varepsilon}{rl}}}{1+\alpha e^{\frac{\varepsilon}{rl}}} & \text{"} \\ \Pr[\mathbf{B}[v_1] = 1 | v_1] = \frac{1}{1+\alpha^3} & \text{if } i \in 2n + 1 \\ \Pr[\mathbf{B}[v_2] = 0 | v_1] = \frac{\alpha e^{\frac{\varepsilon}{rl}}}{1+\alpha e^{\frac{\varepsilon}{rl}}} & \text{"} \end{cases} \quad (17)$$

$$\begin{aligned} \frac{\Pr[\mathbf{B}[v_1]]}{\Pr[\mathbf{B}[v_2]]} &= \frac{\prod_{i \in [d]} \Pr[\mathbf{B}[i]|v_1]}{\prod_{i \in [d]} \Pr[\mathbf{B}[i]|v_2]} \\ &= \frac{\prod_{i \in 2n} \Pr[\mathbf{B}[i]|v_1]}{\prod_{i \in 2n} \Pr[\mathbf{B}[i]|v_2]} \times \frac{\prod_{i \in 2n+1} \Pr[\mathbf{B}[i]|v_1]}{\prod_{i \in 2n+1} \Pr[\mathbf{B}[i]|v_2]} \\ &\leq \left(\frac{\Pr[\mathbf{B}[v_1] = 1|v_1] \Pr[\mathbf{B}[v_2] = 0|v_1]}{\Pr[\mathbf{B}[v_1] = 1|v_2] \Pr[\mathbf{B}[v_2] = 0|v_2]} \right)_{i \in 2n}^{\frac{rl}{2}} \times \\ &\quad \left(\frac{\Pr[\mathbf{B}[v_1] = 1|v_1] \Pr[\mathbf{B}[v_2] = 0|v_1]}{\Pr[\mathbf{B}[v_1] = 1|v_2] \Pr[\mathbf{B}[v_2] = 0|v_2]} \right)_{i \in 2n+1}^{\frac{rl}{2}} \\ &= \left(\left(\frac{\alpha}{1+\alpha} \right) \cdot \left(\frac{\alpha e^{\frac{\varepsilon}{rl}}}{1+\alpha e^{\frac{\varepsilon}{rl}}} \right) \right)^{\frac{rl}{2}} \left(\left(\frac{1}{1+\alpha^3} \right) \cdot \left(\frac{\alpha e^{\frac{\varepsilon}{rl}}}{1+\alpha e^{\frac{\varepsilon}{rl}}} \right) \right)^{\frac{rl}{2}} \\ &= e^{\varepsilon} \end{aligned} \quad (18)$$

□

C. Conducting federated learning over randomized data

LDPFL uses a fully connected deep neural network as the client model during federated learning. As the randomized data are extensively long 1-D vectors, a fully connected model is more flexible towards high performance. After declaring the FL setup, the clients feed the randomized binary vectors as inputs to an FL setup. During this step, we assume that all examples are independent and identically distributed (i.i.d.). We also assume that clients do not collude with one another. This is a practical assumption as, in an FL setup, the clients

directly communicate with the FL server making the clients unaware of other clients of the server. Besides, the clients are assumed to be semi-honest (honest but curious); hence, they do not feed adversarial examples to the FL setup leading to undesirable model performance.

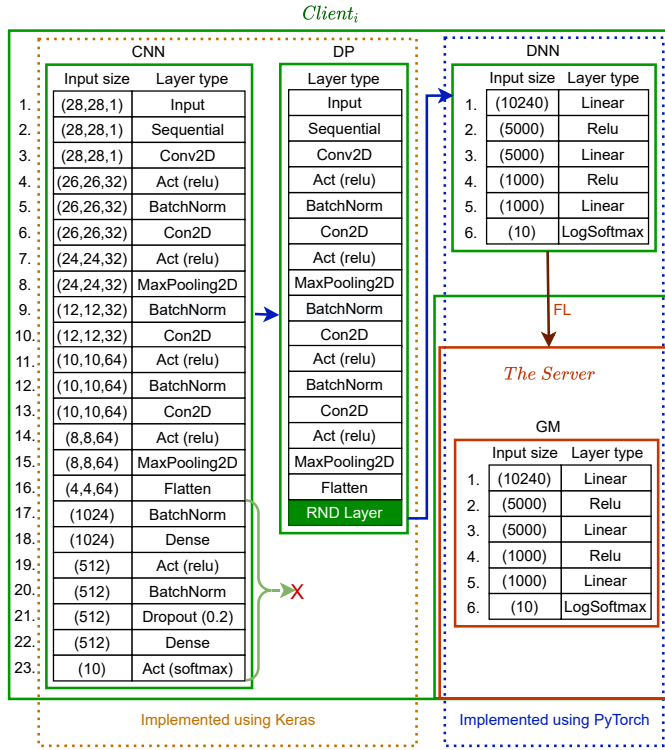


Figure 3: LDPFL architecture used for the MNIST dataset. Act = Activation, BatchNorm = Batch normalization, RND layer= Randomization layer, FL = Federated learning.

As shown in Figure 1, after initialization of the local models, all clients train a local model (as represented by DNN in the figure) using the randomized inputs for a certain number of local epochs and transfer the trained model parameters to the federating server. The clients may intermittently connect and disconnect from the server. Hence, we can expect only a particular portion of the clients to communicate with the server during one round. The federating server (represented by GM in the figure) applies federated parameter averaging on all the parameters received from the clients during the current round. Next, GM sends the federated parameters back to the clients contributed during the corresponding round for model federating. Since LDPFL uses local differential privacy at each client and the data distribution among the clients is IID, the final privacy budget consumption is the maximum of all privacy budgets used by each client ($\max\{\varepsilon_1, \varepsilon_2, \dots, \varepsilon_n\} - DP$).

D. Algorithm for LDPFL

Algorithm 1 shows the steps of LDPFL in conducting differentially private federated learning. It shows the flow of steps in producing randomized inputs and using them in federated learning.

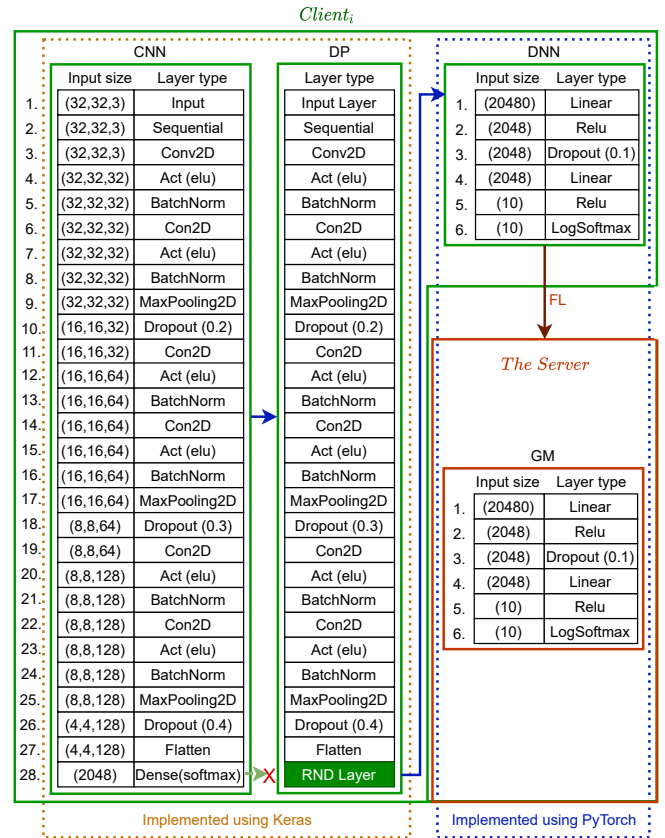


Figure 4: LDPFL architecture used for the CIFAR10 and SVHN datasets. Act = Activation, BatchNorm = Batch normalization, RND layer= Randomization layer, FL = Federated learning. **Note:** When the input dataset is FMNIST, the CNN layer 1 size was changed to 28x28x1, and the DNN and GM layer 1 sizes were changed to 11520.

IV. RESULTS AND DISCUSSION

This section provides the details of experimental configurations, experiments, results, and discussions on them. First, we define two exemplary configurations for LDPFL to answer different levels of input data complexity. Next, we test the model performance under different settings followed by a performance comparison as explained below to highlight the advantages of LDPFL over existing approaches. To test LDPFL, we used the MNIST [29] dataset, the CIFAR10 dataset [10], the SVHN dataset [30], and the FMNIST dataset [31]. MNIST and CIFAR10 are two frequently used benchmarked datasets used for performance testing in deep learning [9], [10]. Regarding the complexity of model training, CIFAR10 is a much more complex dataset to be trained than MNIST. Hence, these two datasets introduce a balanced experimental setting for LDPFL performance testing. However, the two datasets (MNIST and CIFAR10) have a limited number of examples of 70,000 and 60,000 images, respectively. The proposed setting of LDPFL needs a large enough representative dataset to fully train the stand-alone CNN models (represented by CNN in Figure 1) located at each client. Hence, to test LDPFL for a large number of clients, an extensive dataset is necessary to enable

all clients to have a large enough partition of the dataset. We solved this by using SVHN, a recently developed large dataset with 600,000 images that is also popular for performance analysis of deep learning, especially during scalability testing. We used the FMNIST dataset for the performance comparison of LDPFL against previous approaches utilizing the benchmarking data produced by a previous study [14]. We used a MacBook pro-2019 computer for all experiments. It has a processing unit of 2.4 GHz 8-Core Intel Core i9, a memory of 32 GB 2667 MHz DDR4, a graphics memory of AMD Radeon Pro 5500M 8 GB.

A. LDPFL architectural configurations and datasets used during the experiments

We used two LDPL architectural configurations to obtain high performance under the different dynamics of the datasets used, as the correct configuration leads to high model quality [28]. Figure 3 shows the architecture used for the MNIST dataset. As shown in Figure 4, we used a comparably complex configuration for CIFAR10, FMNIST, and SVHN as they are more complex datasets compared to MNIST. Figures 3 and 4 show the flow of modules in LDPFL, layer types used in the networks, the input size of each layer, and the layer order from top to bottom. The input size of a particular layer also indicates the output size of the previous layer. The resolution of an image in FMNIST is $28 \times 28 \times 1$ was different from image resolution ($32 \times 32 \times 3$) in CIFAR10 and SVHN. Hence, we made necessary modifications (discussed in Sections IV-A1 and IV-E) to the architecture in Figure 4 to accommodate the change in the input size when LDPFL was conducted under FMNIST. As shown in Figures 3 and 4 we used the Python Keras API [32] to implement the CNN and DP modules. The federated learning module of LDPFL was implemented using the PyTorch API [33]. We chose Keras and PyTorch based on their competitive advantages on the fast implementation of each module of LDPFL.

We identified the most suitable settings for the CNN and DNN configurations (refer to Figures 3 and 4) using a preliminary analysis of the input datasets. The settings which returned the most satisfactory performance under the given constraints were recorded and utilized during the experiments. The details about the preliminary analysis were omitted from this paper to reduce redundancy and maintain the paper’s clarity and readability.

1) *CNN configurations:* The images in the MNIST dataset have a resolution of $28 \times 28 \times 1$ (one channel), which are size-normalized and centered [29]. Hence, the input layer size of the CNN used for MNIST is $28 \times 28 \times 1$ (refer to Figure 3. Convolution layers no. 3 and no. 6 use $32, 3 \times 3$ filters with stride 1, whereas convolution layers no.10 and no.13 use $64, 3 \times 3$ filters with stride 1. We used a kernel regularizer of regularizers.l2(weight_decay = $1e-4$) for all convolution layers. Both max-pooling layers (layers no. 8 and no.15) use 2×2 max pools. All batch normalization layers (layer numbers 5,9,12,17, and 20) use “axis=-1”.

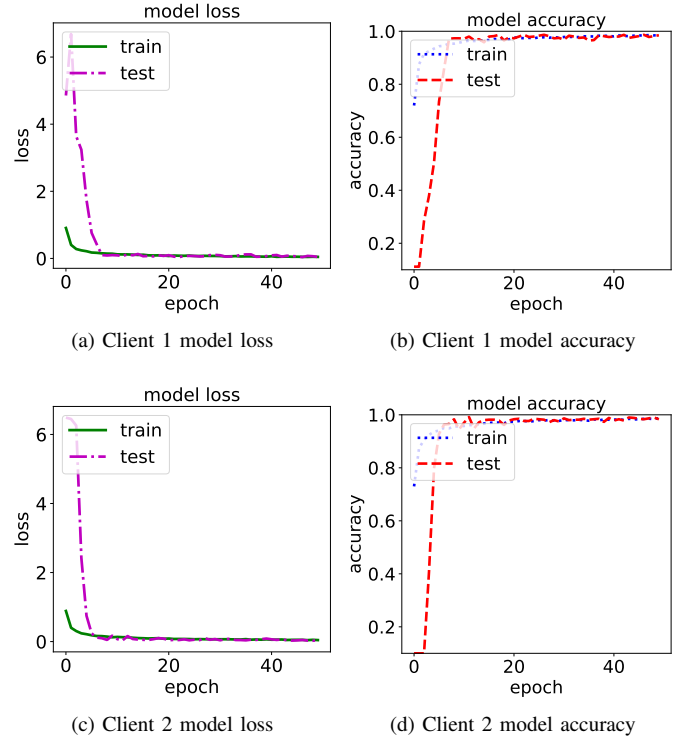


Figure 5: MNIST local model (refer to CNN in Figures 1 and 3) performance

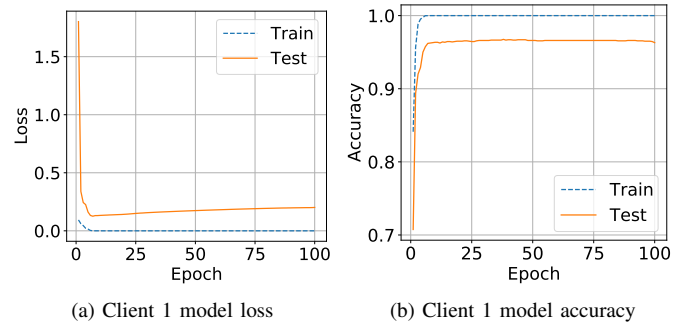


Figure 6: MNIST global model (refer to GM in Figures 1 and 3) performance

The images in the CIFAR10 and SVHN datasets have a resolution of $32 \times 32 \times 3$, which are size-normalized and centered [29]. Hence, the input layer size of the CNNs used for CIFAR10 and SVHN is $32 \times 32 \times 3$ (refer to Figure 4). Convolution layers no. 3 and no. 6 use $32, 3 \times 3$ filters with stride 1, convolution layers no.11 and no.14 use $64, 3 \times 3$ filters with stride 1, and convolution layers no.19 and no.22 use $128, 3 \times 3$ filters with stride 1. All three max-pooling layers (layers no. 9, no.17, and no.25) use 2×2 max pools. The image resolution of FMNIST images is $28 \times 28 \times 1$. Hence, only the input layer size of the CNN (refer to Figure 4) was changed to $28 \times 28 \times 1$ while keeping all other settings of the local CNN architecture unchanged.

B. The data distribution among clients

We investigated the effect of the number of clients on LDPFL by repeating the experiments under a different number of clients every time. To ensure that the number of records is equal throughout all experiments, we first split the total number of records into groups having equal numbers of records according to the highest number of clients – N_h (that the LDPFL was going to be tested on). Hence, during each experiment, a particular client holds a total of $\frac{T_r}{N_h}$ records, where T_r is the total number of records.

C. Client CNN training with image augmentation

We used the same configurations for training the CNN (at the client) module for all datasets. First, the main datasets (MNIST, CIFAR10, FMNIST, and SVHN) were split into training and testing. We used 60000, 50000, 60000, and 451461 training samples and 10000, 10000, 10000, and 79670 testing samples, and N_h was set to 2, 2, 10, and 100 under MNIST, CIFAR10, FMNIST, and SVHN, respectively. Hence, each client had 30000, 25000, 6000, and 4514 data samples for training, and 5000, 5000, 1000, and 796 testing samples under MNIST, CIFAR10, FMNIST, and SVHN, respectively. Each client used 90% of local data for training and 10% for testing. All clients used image augmentation to maintain a high local model performance and robustness under a low number of data samples. For this task, we used "ImageDataGenerator" (from keras.preprocessing.image) with rotation_range=15, width_shift_range=0.1, and height_shift_range=0.1. We used RMSprop(lr=0.001,decay=1e-6) optimizer for local CNN training with a batch size of 64. We schedule the learning rate to drop from 0.001 to 0.0005 after the 75th epoch and 0.0003 after the 100th epoch to enhance the model performance further. All CNNs were trained for 50 epochs. Figures 5 and 7 show the two CNN client model performances under MNIST and CIFAR10, respectively. Figure 12 shows the CNN model performance of a randomly chosen one of the 10 clients under FMNIST. From the 100 dataset splits of SVHN, we only considered a maximum of 50 clients as it provided enough evidence to understand the LDPFL performance patterns against the increasing number of clients while enabling the LDPFL to converge under adequate time in the MacBook computer (which was used for the experiments). Figure 9 shows the CNN model performance of a randomly chosen one of the 50 clients. The figures show that the configurations chosen for the client CNN models under each dataset generate good model performance.

D. Data randomization for differentially private FL

After the client CNN models converge, each input is fed to the converged model, and the output of the flattened layer (refer to layer number 16 of Figure 3 and layer number 27 of Figure 4) is then randomized according to Section III-B. This is continued to all inputs of the corresponding client. As the model was already trained on the inputs, the flattened outputs can maintain a high correlation to the corresponding inputs, and the randomized data can appropriately preserve the input

characteristics leading to good classification accuracy. During the randomization, we maintained m , n , α , and ϵ at 4, 5, 10, and 0.5, respectively. With the sign bit, each digit in the flattened output is encoded to 10-bit $l = (m + n + 1)$ binary representation. m and n can be selected based on the scale of the inputs to binary encoding. A higher number of bits for n can be selected to represent the fraction part for more precision, whereas the number of bits used for m represents the range of integers that can be represented. As the inputs to the CNN are normalized (all image pixel values are divided by 255), it can be observed that the flatten output produces values between 0 and 1. Hence, we selected the corresponding values (4 and 5) for m and n . Although increasing n could improve the precision to produce high utility, it also increases the sensitivity of the encoded binary string requiring more randomization. The output of layer number 16 of Figure 3 produces a $r = 1024$ digit vector, and the output of layer number 27 of Figure 4 produces a $r = 2048$ digit vector. However, during FMNIST, layer number 27 of Figure 4 produces a $r = 1152$ digit vector, due to image resolution differences as mentioned in Section IV-A1. Consequently, binary encoding of the outputs from the flattening layers produces binary vectors of length $rl = 10240$ under MNIST and $rl = 20480$ under CIFAR10 and SVHN, and $rl = 11520$ under FMNIST. Since the sensitivity of the encoded binary strings are equal to their lengths (rl), the probability of randomization of the binary strings can be written as $p = \frac{e^{\epsilon/10240}}{1+e^{\epsilon/10240}}$ for MNIST, $p = \frac{e^{\epsilon/20480}}{1+e^{\epsilon/20480}}$ for CIFAR10 and SVHN, and $p = \frac{e^{\epsilon/11520}}{1+e^{\epsilon/11520}}$ for FMNIST. Hence, we maintain epsilon at 0.5, as increasing ϵ within the acceptable limits (e.g. $0 < \epsilon \leq 10$) has a negligible impact on the randomization probability. α provides additional flexibility towards maintaining the probability of transmitting the 0 bits in their original state. By maintaining α at a constant value of 10, we ensure that the binary string randomization dynamics are kept uniform during all experiments to observe unbiased results.

E. Federated learning over randomized data

The part of the Figures 3 and 4 enclosed by the blue dotted square shows the configurations of the DNNs used in the FL setup of LDPFL. The number of neurons in the first layer (of the DNNs) is equivalent to the number of digits in the randomized binary vectors (under the corresponding dataset). The DNNs are trained solely on the randomized binary strings (generated according to Section IV-D); hence, enabling differentially private federated learning as a result of the postprocessing invariance property of DP. Consequently, the converged FL model provides ϵ -DP. In the FL setup with more than two clients (during the experiments under FMNIST and SVHN), we dropped the updates from a randomly chosen client every round to simulate the intermittent client dropouts in a real-world setting. However, many clients (realistically more than one) can intermittently drop out in real-world scenarios, requiring longer FL training rounds before model convergence. Under MNIST, all the clients use Adam

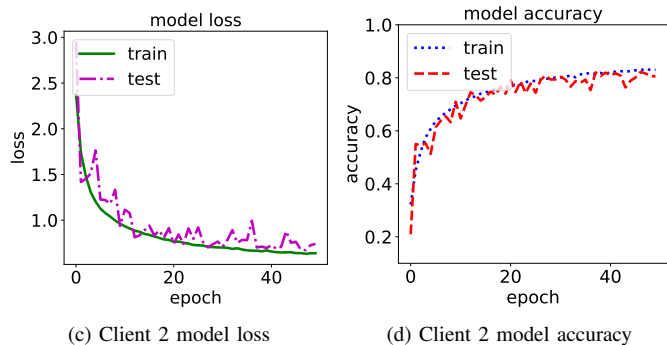
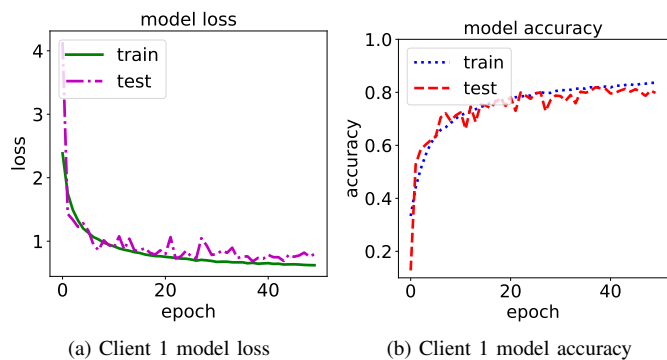


Figure 7: CIFAR10 local model (refer to CNN in Figures 1 and 4) performance

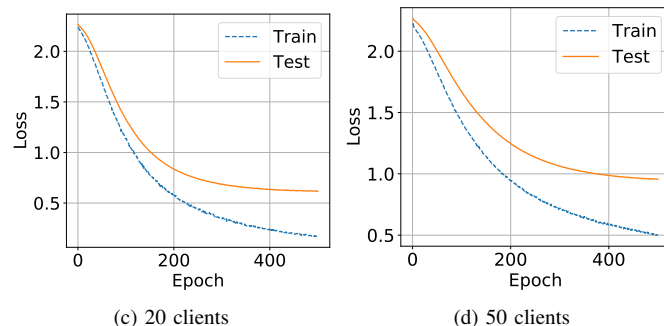
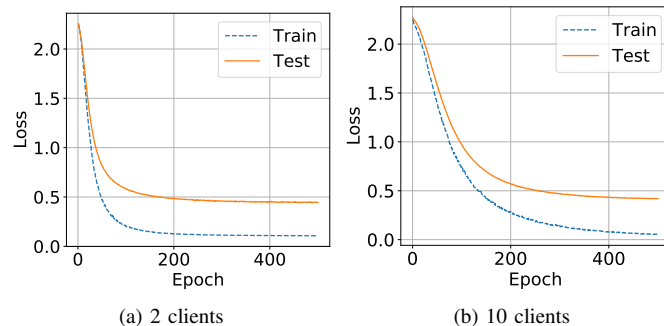


Figure 10: SVHN global model (refer to GM in Figure 1 and 4) loss under different numbers of clients

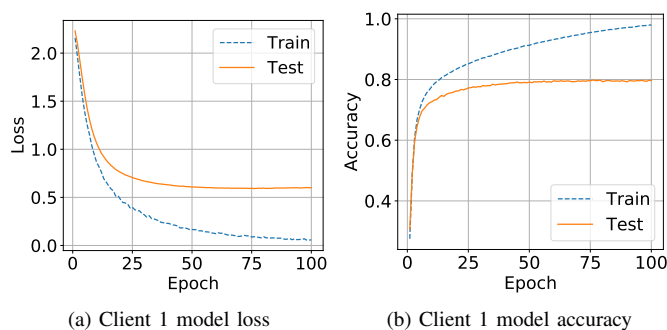


Figure 8: CIFAR10 global model (refer to GM in Figures 1 and 4) performance

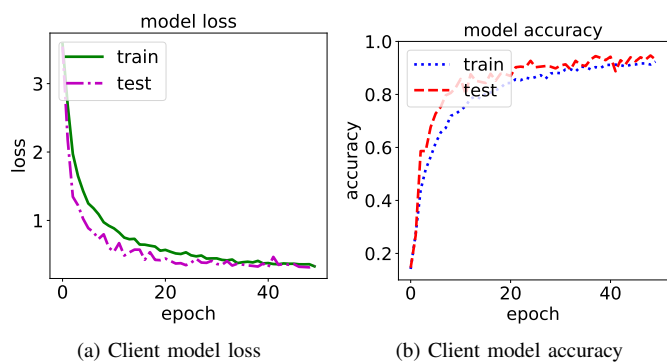
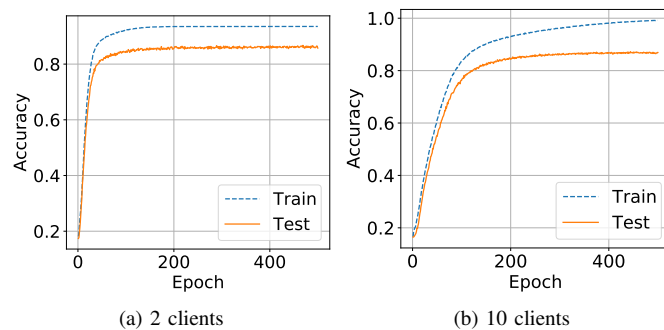


Figure 9: SVHN local model performance of a client (randomly selected - refer to CNN in Figures 1 and 4)

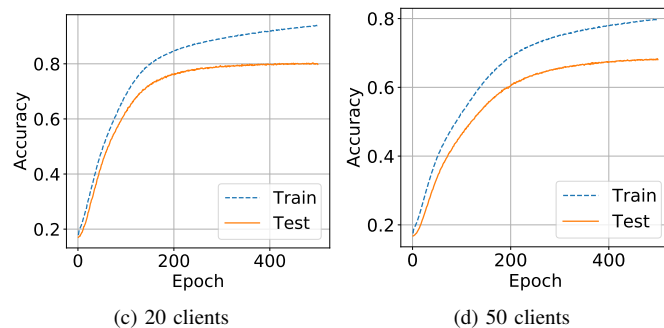


Figure 11: SVHN global model (refer to GM in Figures 1 and 4) accuracy under different numbers of clients

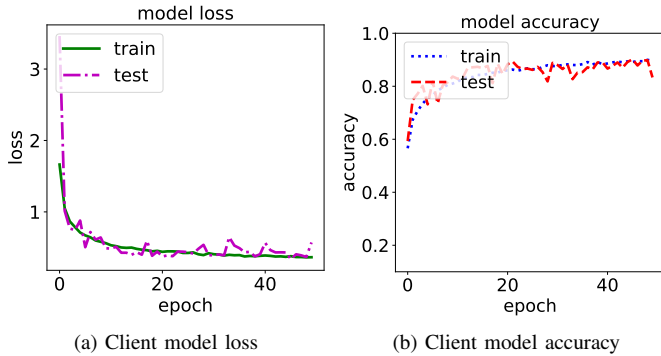


Figure 12: FMNIST local model performance of a client (randomly selected - refer to CNN in Figures 1 and 4)

(betas=(0.9, 0.999), eps=1e-08) optimizer, whereas, under CIFAR10, FMNIST, and SVHN, all the clients use stochastic gradient descent (SGD) optimizer for local model learning with a learning rate of 0.001 and a batch size of 64. FL process starts with the central server randomly initializing the parameters and distributing them to the clients to initialize their local models with the initial parameters. Next, each client runs the local DNNs for 20 epochs and sends the trained parameters to the server. The server conducts federated averaging on all parameter matrices of the clients who contributed during the current round. Next, the server forwards the aggregated parameters to the clients, and the clients update the states of their local models with the federated parameters sent by the server. The execution of client model training for 20 epochs, model federation, and model state update with federated parameters is considered as 1 round of FL. We conduct 100 such rounds of FL to investigate the model convergence in LDPFL under MNIST and CIFAR10. However, FL takes more time for convergence when there are many clients. Hence, we used 500 FL rounds for LDPFL performance analysis under SVHN. In the case of FMNIST, we run FL for 80 rounds to replicate the settings of a previous study [14], which we utilize for benchmarking.

1) *LDPFL model performance*: Figures 6 and 8 show the performance of the final LDPFL models under MNIST and CIFAR10, respectively. LDPFL generates good model performance under both datasets. As LDPFL uses the fully trained CNN to generate a subsequent training dataset for the DP federated learning step of LDPFL, it is essential to have a good client CNN model performance. In the proposed setting, a client represents a considerably large-scale entity (e.g. a bank, a hospital). Hence, we assume that each client has a large enough dataset locally to train the local CNN models to produce good CNN model performance. Thus, the subsequent dataset generated by the CNN model inherits the distribution characteristics influenced by the CNN model. Besides, the extensive feature space generated during the feature flattening (long 1-D binary vectors) step leads to high utility preservation.

Figures 9a and 9b show the model loss and accuracy con-

vergence of LDPFL under different numbers of clients. Figure 13 provides a comparison of the testing accuracy convergence of the LDPFL model under different client numbers. The higher the number of clients, the higher the time necessary for model convergence. We can also notice that the accuracy slightly decreases when the number of clients increases. This is because each client has a lower number of tuples and produces a CNN with slightly less generalizability. Consequently, each client applying LPD locally while maintaining local data representations can entail high randomization diversity. The higher the number of clients, the higher the randomization diversity; hence, requiring more data instances per client to prevent from dropping accuracy. However, because the clients in LDPFL maintain the local data distributions by utilizing a locally converged model (with good performance) on the input data, LDPFL provides a better approach to maintain utility under complex datasets than other LDP approaches when there are many clients.

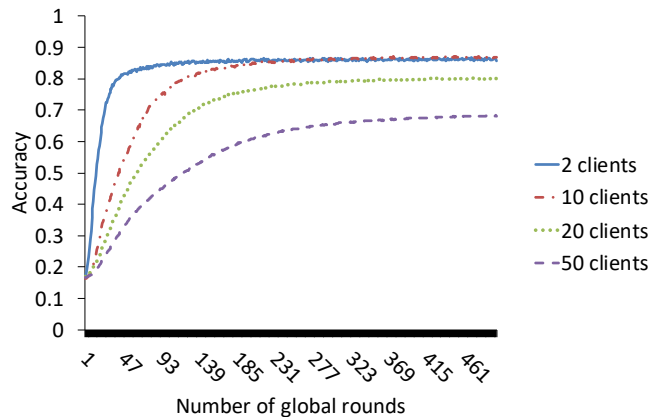


Figure 13: SVHN Global model (refer to GM in Figures 1 and 4) test accuracy comparison

2) *Performance comparison of LDPFL against existing approaches*: For the performance comparison, we followed the benchmarking used in a previous study [14] on an approach named LDP-Fed that imposes α -CLDP (a generalization of LDP [17]) on federated learning. We compare the results of LDPFL against 4 previous approaches; (1) Non-private, (2) Secure multi-party computing (SMC) [6], [14], (3) Differentially private stochastic gradient descent (DPSGD) [10], [14], and (4) α -Condensed Local Differential Privacy for Federated Learning (α -CLDP-Fed) [14], [17]. These four approaches consider the k-Client selection protocol in which 9 client updates will be considered for the federation in every round [14]. For benchmarking [14] set α of α -CLDP-Fed to 1.0, and the privacy parameters (e.g. ϵ and δ) of the other three approaches are set accordingly to match with $\alpha = 1.0$ [14], [17]. We use the same default privacy parameters explained in Section IV-D for LDPFL (refer to Section IV-D for the primary factors that influence value assignments for the privacy parameters). However, LDPFL enforces much stronger level of privacy compared to all other approaches in Table I. The table provides

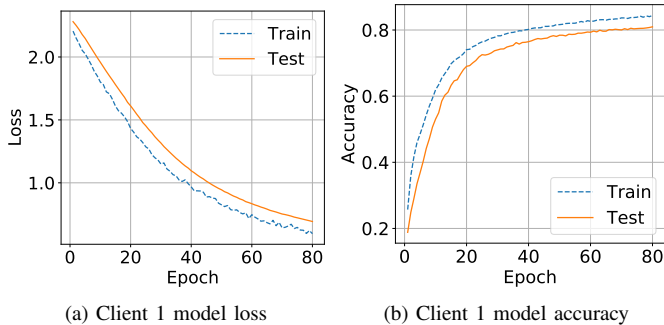


Figure 14: FMNIST global model (refer to GM in Figures 1 and 4) performance

the comparison between all 5 methods. The accuracy was generated on the FMNIST dataset. For LDPFL, we considered 9 randomly chosen client updates out of 10. The model convergence of LDPFL for FMNIST is shown in Figures 14. The accuracy values of Table I are generated after 80 rounds of the federation. As shown in the table, LDPFL generates an accuracy greater than that of DPSGD while enforcing the strictest privacy among all 5 approaches. Hence, we can conclude that LDPFL provides an overall better performance while providing the best balance between privacy and utility.

Table I: Comparison of LDPFL against the existing methods

Method	Efficiency (compared to baseline)	Privacy Model	Privacy Model strength	Trusted Party Requirement	Accuracy (after 80 rounds with 9 client updates every round)
Non-private	Baseline	NA	NA	RQ	~90%
SMC	Low	NA	ND	RQ	~90%
DPSGD	High	(ϵ, δ) -DP	Basic	RQ	~80%
α -CLDP-Fed	High	α -CLDP	Moderate	NR	~85.28% - 86.93%
LDPFL	High	ϵ -LDP	High	NR	~81%

V. RELATED WORK

Federated learning (FL) tries to solve privacy issues in distributed machine learning by introducing a model-to-data approach where data resides in the data owners' computers. Although this approach provides a certain level of privacy for the distributed data, FL is vulnerable to model inference-based advanced adversarial attacks such as membership inference, distribution estimation attacks, training data reconstruction attacks, and model inversion attacks [34]–[38]. These attacks try to exploit model information to learn about user data. Different approaches in privacy-preserving data mining (PPDM) were utilized to overcome these privacy issues in FL. These approaches can be broadly categorized into encryption-based (cryptographic) [6] and data modification-based (perturbation) [4].

Cryptographic approaches look at how secure aggregation of parameters can be conducted at the FL server. Cryptographic approaches on FL showed high effectiveness in providing high

security and privacy. The most widely adapted cryptographic approach for secure aggregation is secure multi-party computation (MPC) [7]. MPC enables the secure evaluation of a function on private data (also called secret shares) distributed among multiple parties who do not trust each other [6]. The requirement of a trusted party (e.g. VerifyNet [39], and VeriFL [40]) or the requirement of a considerably high number of communications (e.g. Bonawitz et al.'s approach [6] and Bell et al.'s approach [41]) are two of the fundamental problems of most of the existing MPC approaches for FL [6]. Besides, the existing MPC approaches show vulnerability towards advanced adversarial attacks such as backdoor attacks [42]. Homomorphic encryption (HE) is the other frequently adapted cryptographic approach for the secure aggregation of parameters in FL. HE enables algebraic operations over encrypted data to produce a ciphertext that can be decrypted to obtain the algebraic outcome on the original plaintext with security and privacy [43]. However, scalability has been a major challenge of HE. The latest approaches, such as BatchCrypt, try to introduce less complex HE-based solutions for secure FL parameter aggregation [44]. Besides, the distributed setting makes them infeasible for large-scale scenarios due to the low efficiency of such approaches [19], [45].

Among different data perturbation techniques for FL, the approaches that satisfy differential privacy are more widely utilized in FL due to DP's strong privacy guarantees [4]. The existing research towards DP approaches for FL focuses on maintaining a balance between privacy and the model performance (e.g. convergence and utility) [4]. Both global differential private (GDP) approaches [8], [46] and local differential private (LDP) [14], [47] approaches were introduced to FL [4]. GDP approaches focus on privately learning the algorithm (e.g. SGD) [8], [48], whereas LDP approaches [14], [47] focus on randomizing the data inputs to the algorithm (it can be the direct randomization of user inputs or randomization of the model parameters before sending them to the aggregator) to learn on randomized data. Robin et al.'s approach [8] and Asoodeh et al.'s approach [46] are two of the GDP approaches for FL, whereas LDP-Fed [14] and Seif et al.'s approach [47] are two LDP approaches. The primary issue of most GDP approaches is the requirement of a trusted aggregator. These approaches focus more on privacy leaks among the clients [8], [46]. By either randomizing user inputs or parameters before sending them to the aggregator, LDP-based approaches provide a stricter privacy setting that tries to avoid privacy leaks among the clients and between the clients and the server [14], [47]. However, existing LDP approaches often consume unreliable privacy budgets (ϵ) to produce good accuracy or do not produce a high accuracy compared to GDP approaches. Hence, there is a significant imbalance between privacy and utility of LDP approaches for FL. It is essential to develop new LDP approaches to answer this challenge.

VI. CONCLUSION

We proposed a utility enhancing local differentially private approach (named LDPFL) for federated learning. The

¹NA: Not available, ND: Not defined, Basic: basic DP, Moderate: not as strong as LDP but better than basic DP, High: satisfies strong LDP guarantees.

proposed approach provides high testing accuracy (e.g. 96%) under strict privacy settings (e.g. $\epsilon = 0.5$). LDPFL achieved an accuracy of 96%, 80%, and 85% at $\epsilon = 0.5$ when there are two clients under MNIST, CIFAR10, and SVHN, respectively. The use of a fully trained model to filter and flatten the input features to generate long binary vectors from the flattening process allows high utility preservation in the proposed approach. Besides, the LDP approach provides high utility preservation towards extensive binary vector randomization by randomizing one half of the binary string differently from the other half, enabling high bit preservation on randomized binary strings. The use of local differential privacy provides LDPFL conducting efficient federated learning under untrusted settings (e.g. with untrusted clients and an untrusted server) while preserving high privacy. Besides, benchmarking suggests that LDPFL is preferred when high utility is required under strict privacy notions.

ACKNOWLEDGMENT

The work has been supported by the Cyber Security Research Centre Limited whose activities are partially funded by the Australian Government's Cooperative Research Centres Programme.

REFERENCES

- [1] P. C. M. Arachchige, P. Bertok, I. Khalil, D. Liu, S. Camtepe, and M. Atiquzzaman, "Local differential privacy for deep learning," *IEEE Internet of Things Journal*, vol. 7, no. 7, pp. 5827–5842, 2019.
- [2] T. Li, A. K. Sahu, A. Talwalkar, and V. Smith, "Federated learning: Challenges, methods, and future directions," *IEEE Signal Processing Magazine*, vol. 37, no. 3, pp. 50–60, 2020.
- [3] Z. Wang, M. Song, Z. Zhang, Y. Song, Q. Wang, and H. Qi, "Beyond inferring class representatives: User-level privacy leakage from federated learning," in *IEEE INFOCOM 2019-IEEE Conference on Computer Communications*. IEEE, 2019, pp. 2512–2520.
- [4] K. Wei, J. Li, M. Ding, C. Ma, H. H. Yang, F. Farokhi, S. Jin, T. Q. Quek, and H. V. Poor, "Federated learning with differential privacy: Algorithms and performance analysis," *IEEE Transactions on Information Forensics and Security*, vol. 15, pp. 3454–3469, 2020.
- [5] Y. Zhang, G. Bai, X. Li, C. Curtis, C. Chen, and R. K. Ko, "Privcoll: Practical privacy-preserving collaborative machine learning," in *European Symposium on Research in Computer Security*. Springer, 2020, pp. 399–418.
- [6] K. Bonawitz, V. Ivanov, B. Kreuter, A. Marcedone, H. B. McMahan, S. Patel, D. Ramage, A. Segal, and K. Seth, "Practical secure aggregation for privacy-preserving machine learning," in *proceedings of the 2017 ACM SIGSAC Conference on Computer and Communications Security*, 2017, pp. 1175–1191.
- [7] H. Fereidooni, S. Marchal, M. Miettinen, A. Mirhoseini, H. Möllering, T. D. Nguyen, P. Rieger, A.-R. Sadeghi, T. Schneider, H. Yalame *et al.*, "Safelearn: secure aggregation for private federated learning," in *2021 IEEE Security and Privacy Workshops (SPW)*. IEEE, 2021, pp. 56–62.
- [8] R. C. Geyer, T. Klein, and M. Nabi, "Differentially private federated learning: A client level perspective," *arXiv preprint arXiv:1712.07557*, 2017.
- [9] R. Shokri and V. Shmatikov, "Privacy-preserving deep learning," in *Proceedings of the 22nd ACM SIGSAC conference on computer and communications security*. ACM, 2015, pp. 1310–1321.
- [10] M. Abadi, A. Chu, I. Goodfellow, H. B. McMahan, I. Mironov, K. Talwar, and L. Zhang, "Deep learning with differential privacy," in *Proceedings of the 2016 ACM SIGSAC Conference on Computer and Communications Security*. ACM, 2016, pp. 308–318.
- [11] X. Xiao and Y. Tao, "Output perturbation with query relaxation," *Proceedings of the VLDB Endowment*, vol. 1, no. 1, pp. 857–869, 2008.
- [12] P. Kairouz, S. Oh, and P. Viswanath, "Extremal mechanisms for local differential privacy," in *Advances in neural information processing systems*, 2014, pp. 2879–2887.
- [13] L. Sun, J. Qian, X. Chen, and P. S. Yu, "Ldp-fl: Practical private aggregation in federated learning with local differential privacy," *arXiv preprint arXiv:2007.15789*, 2020.
- [14] S. Truex, L. Liu, K.-H. Chow, M. E. Gursoy, and W. Wei, "Ldp-fed: Federated learning with local differential privacy," in *Proceedings of the Third ACM International Workshop on Edge Systems, Analytics and Networking*, 2020, pp. 61–66.
- [15] J. A. Fox, *Randomized response and related methods: Surveying Sensitive Data*. SAGE Publications, 2015, vol. 58.
- [16] T. Wang, J. Blocki, N. Li, and S. Jha, "Locally differentially private protocols for frequency estimation," in *26th {USENIX} Security Symposium ({USENIX} Security 17)*, 2017, pp. 729–745.
- [17] M. E. Gursoy, A. Tamersoy, S. Truex, W. Wei, and L. Liu, "Secure and utility-aware data collection with condensed local differential privacy," *IEEE Transactions on Dependable and Secure Computing*, 2019.
- [18] H. B. McMahan, E. Moore, D. Ramage, and B. A. y Arcas, "Federated learning of deep networks using model averaging," 2016.
- [19] Q. Yang, Y. Liu, T. Chen, and Y. Tong, "Federated machine learning: Concept and applications," *ACM Transactions on Intelligent Systems and Technology (TIST)*, vol. 10, no. 2, p. 12, 2019.
- [20] M. Chamikara, P. Bertok, D. Liu, S. Camtepe, and I. Khalil, "An efficient and scalable privacy preserving algorithm for big data and data streams," *Computers & Security*, vol. 87, p. 101570, 2019.
- [21] T.-H. H. Chan, M. Li, E. Shi, and W. Xu, "Differentially private continual monitoring of heavy hitters from distributed streams," in *International Symposium on Privacy Enhancing Technologies Symposium*. Springer, 2012, pp. 140–159.
- [22] Ú. Erlingsson, V. Pihur, and A. Korolova, "Rappor: Randomized aggregatable privacy-preserving ordinal response," in *Proceedings of the 2014 ACM SIGSAC conference on computer and communications security*. ACM, 2014, pp. 1054–1067.
- [23] S. L. Warner, "Randomized response: A survey technique for eliminating evasive answer bias," *Journal of the American Statistical Association*, vol. 60, no. 309, pp. 63–69, 1965.
- [24] Y. Wang, X. Wu, and D. Hu, "Using randomized response for differential privacy preserving data collection," in *EDBT/ICDT Workshops*, vol. 1558, 2016.
- [25] Z. Qin, Y. Yang, T. Yu, I. Khalil, X. Xiao, and K. Ren, "Heavy hitter estimation over set-valued data with local differential privacy," in *Proceedings of the 2016 ACM SIGSAC Conference on Computer and Communications Security*. ACM, 2016, pp. 192–203.
- [26] M. Bun and T. Steinke, "Concentrated differential privacy: Simplifications, extensions, and lower bounds," in *Theory of Cryptography Conference*. Springer, 2016, pp. 635–658.
- [27] J. Zhao, Y. Chen, and W. Zhang, "Differential privacy preservation in deep learning: Challenges, opportunities and solutions," *IEEE Access*, vol. 7, pp. 48901–48911, 2019.
- [28] J. Schmidhuber, "Deep learning in neural networks: An overview," *Neural networks*, vol. 61, pp. 85–117, 2015.
- [29] Y. LeCun, L. Bottou, Y. Bengio, and P. Haffner, "Gradient-based learning applied to document recognition," *Proceedings of the IEEE*, vol. 86, no. 11, pp. 2278–2324, 1998.
- [30] P. Sermanet, S. Chintala, and Y. LeCun, "Convolutional neural networks applied to house numbers digit classification," in *Proceedings of the 21st International Conference on Pattern Recognition (ICPR2012)*. IEEE, 2012, pp. 3288–3291.
- [31] H. Xiao, K. Rasul, and R. Vollgraf, "Fashion-mnist: a novel image dataset for benchmarking machine learning algorithms," *arXiv preprint arXiv:1708.07747*, 2017.
- [32] F. Chollet *et al.*, "Keras: Deep learning library for theano and tensorflow," *URL: https://keras.io/k*, vol. 7, no. 8, 2015.
- [33] A. Paszke, S. Gross, F. Massa, A. Lerer, J. Bradbury, G. Chanan, T. Killeen, Z. Lin, N. Gimelshein, L. Antiga *et al.*, "Pytorch: An imperative style, high-performance deep learning library," *Advances in neural information processing systems*, vol. 32, pp. 8026–8037, 2019.
- [34] K. Yang, Q. Han, H. Li, K. Zheng, Z. Su, and X. Shen, "An efficient and fine-grained big data access control scheme with privacy-preserving policy," *IEEE Internet of Things Journal*, vol. 4, no. 2, pp. 563–571, 2017.
- [35] D. Vatsalan, Z. Sehili, P. Christen, and E. Rahm, "Privacy-preserving record linkage for big data: Current approaches and research challenges," in *Handbook of Big Data Technologies*. Springer, 2017, pp. 851–895.
- [36] M. Fredrikson, S. Jha, and T. Ristenpart, "Model inversion attacks that exploit confidence information and basic countermeasures," in

- Proceedings of the 22nd ACM SIGSAC Conference on Computer and Communications Security*. ACM, 2015, pp. 1322–1333.
- [37] M. Nasr, R. Shokri, and A. Houmansadr, “Machine learning with membership privacy using adversarial regularization,” in *Proceedings of the 2018 ACM SIGSAC Conference on Computer and Communications Security*, 2018, pp. 634–646.
- [38] A. Salem, A. Bhattacharya, M. Backes, M. Fritz, and Y. Zhang, “Updates-leak: Data set inference and reconstruction attacks in online learning,” in *29th {USENIX} Security Symposium ({USENIX} Security 20)*, 2020, pp. 1291–1308.
- [39] G. Xu, H. Li, S. Liu, K. Yang, and X. Lin, “Verifynet: Secure and verifiable federated learning,” *IEEE Transactions on Information Forensics and Security*, vol. 15, pp. 911–926, 2019.
- [40] X. Guo, Z. Liu, J. Li, J. Gao, B. Hou, C. Dong, and T. Baker, “V erifi: Communication-efficient and fast verifiable aggregation for federated learning,” *IEEE Transactions on Information Forensics and Security*, vol. 16, pp. 1736–1751, 2020.
- [41] J. H. Bell, K. A. Bonawitz, A. Gascón, T. Lepoint, and M. Raykova, “Secure single-server aggregation with (poly) logarithmic overhead,” in *Proceedings of the 2020 ACM SIGSAC Conference on Computer and Communications Security*, 2020, pp. 1253–1269.
- [42] E. Bagdasaryan, A. Veit, Y. Hua, D. Estrin, and V. Shmatikov, “How to backdoor federated learning,” in *International Conference on Artificial Intelligence and Statistics*. PMLR, 2020, pp. 2938–2948.
- [43] C. Gentry, *A fully homomorphic encryption scheme*. Stanford university, 2009.
- [44] C. Zhang, S. Li, J. Xia, W. Wang, F. Yan, and Y. Liu, “Batchcrypt: Efficient homomorphic encryption for cross-silo federated learning,” in *2020 {USENIX} Annual Technical Conference ({USENIX}{ATC} 20)*, 2020, pp. 493–506.
- [45] J. So, B. Güler, and A. S. Avestimehr, “Turbo-aggregate: Breaking the quadratic aggregation barrier in secure federated learning,” *IEEE Journal on Selected Areas in Information Theory*, vol. 2, no. 1, pp. 479–489, 2021.
- [46] S. Asoodeh, W.-N. Chen, F. P. Calmon, and A. Özgür, “Differentially private federated learning: An information-theoretic perspective,” in *2021 IEEE International Symposium on Information Theory (ISIT)*. IEEE, 2021, pp. 344–349.
- [47] M. Seif, R. Tandon, and M. Li, “Wireless federated learning with local differential privacy,” in *2020 IEEE International Symposium on Information Theory (ISIT)*. IEEE, 2020, pp. 2604–2609.
- [48] H. B. McMahan, D. Ramage, K. Talwar, and L. Zhang, “Learning differentially private recurrent language models,” *arXiv preprint arXiv:1710.06963*, 2017.